Academic Journal of Science and Technology
ISSN: 2771-3032 | Vol. 11, No. 3, 2024

Design and Strength Check of an Automatic Pneumatic Elevator

Changlin Zhou [1], Junming Zhang [2], Wei Luo [1], Tao Huang [2], Lei Yang [1], Tao Song [1], Rui Liu [1], Xiaolin Luo [1], Ye Yuan [1]

[1] Sichuan ShengNuo Oil and Gas Engineering Technology Servicw Co., LTD, China
[2] Southwest Petroleum University, Chengdu, China

Abstract: The pneumatic elevator is used to replace the manual grabbing and releasing of the tubing, which solves the problems of complicated, easy leakage and the high environmental requirements of the traditional hydraulic elevator. The advantages of the sling are the use of an air pressure drive, remote control, improved safety, and the fact that it can be used in harsh environments. Through the finite element strength analysis, the material of the main bearing parts of the pneumatic elevator is calculated to meet the strength requirements. Through continuous functional testing and load testing, the correctness of the finite element analysis of the pneumatic elevator is verified. The functions of the pneumatic elevator operate normally, and the overall bearing operation is stable, safe, and reliable. The data show that the pneumatic elevator meets the design requirements.

Keywords: Pneumatic Elevator; Structural Design; Finite Element Analysis; Expansion Buckle Sleeve; Strength Check; Experimental Verification.

1. Introduction

In the oil drilling operation, it is necessary to grab and transport the tubing frequently. With the continuous development of oil industry technology, the requirements for operation efficiency, safety, and stability are increasing day by day [1–2]. Although the traditional tubing grabbing equipment meets the operation requirements to a certain extent, it still needs to be improved in terms of operation convenience, level, and safety. As a kind of hoisting equipment based on motor transmission and control technology, the power elevator has shown great application potential in the field of oil drilling and production due to its high efficiency and adaptability, high safety, low maintenance cost, and easy control [3–7]. Therefore, it is of great practical significance and application prospect to design a new type of automatic elevator that combines the elevator with automation technology to realize fast and accurate grasping of the oil pipe, reduce manual operation, and improve operation efficiency and safety [8–12]. In order to save money and improve operation and safety, Sichuan Shengnuo Oil and Gas Engineering Technology Service Co., Ltd. developed a pneumatic elevator based on the structure and technological innovation of hydraulic elevators according to the situation of workover operation equipment in China. Breakthroughs have been made in control technology and successfully applied, with obvious results.

2. Pneumatic Elevator System Parameters

2.1. Pneumatic Elevator Structure Composition

The pneumatic elevator is mainly composed of an elevator frame, pneumatic motor, connector, elevator body, buffer spring, driven shaft, expansion sleeve, guiding shaft, guiding sleeve, and so on. The mechanism is shown in Fig.1. The sling frame has the function of fixing and connecting supports. The left and right wings of the frame are passed through a fixed steel wire to prevent shaking from affecting the neutral of the sling. The pneumatic motor is used as a power source to generate torque, which is transmitted to the connector and then to the lower guider area. The guide area includes the driven shaft, the expansion sleeve, the guide shaft, and the guide sleeve, which plays a guiding and centering role in the buckle process. The thread of the expansion sleeve and the thread of the tubing are screwed together to complete the tubing grasp.

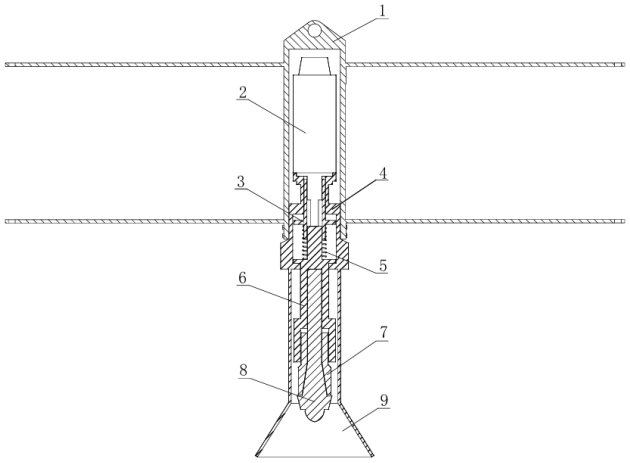

1-hanging card frame; 2-pneumatic motor; 3-connector; 4-lift body; 5-buffer spring;
6-driven shaft; 7- expansion buckle sleeve; 8-guide axis; 9-guide sleeve;
Fig 1. Pneumatic elevator structure diagram

2.2. Technical Parameters of Pneumatic Elevator

The designed pneumatic lifting card requires a weight of less than 200 kg, the maximum lifting weight is 200 kg, and the final design finished product parameters are shown in Table 1. Its maximum diameter is 290 mm at the large end of the guide sleeve. By replacing the guider area, it can adapt to the pull-off and pull-back functions of 23 / 8 ~ 31 / 2 tubing.

Table 1. Design parameters of pneumatic elevator

Parameter name	concrete parameters
Weight	56.4kg
Height	1188mm
Rated power	2.85kw
Rated torque	300N·m
Applicable pipe diameter	23/8~31/2

A pneumatic motor is customized according to the requirements of the pneumatic elevator. Compared with the hydraulic motor, it has the advantages of high working safety, strong adaptability, flexible operation, high efficiency, and energy savings. The specific parameters are shown in Table 2.

Table 2. Pneumatic motor parameters

Parameter name	concrete parameters
Model	6AM-RV-P120.11X
Rated power	2.85kw
Rated torque	300N·m
Rated speed	90rpm
Maximum torque	375N·m
Rotating speed at maximum torque	9rpm
Working pressure	7Bar
Air consumption	3700L/min
Weight	17KG

2.3. Air Pressure System Design

The whole air pressure system is composed of two air ports on the pneumatic motor, which are connected to the spiral variable frequency air compressor system (with gas storage tank, cold dryer, drain, and filter) through the high-pressure air pump hose and controlled by a three-position, five-way manual control valve. The control principle is shown in Fig. 2.

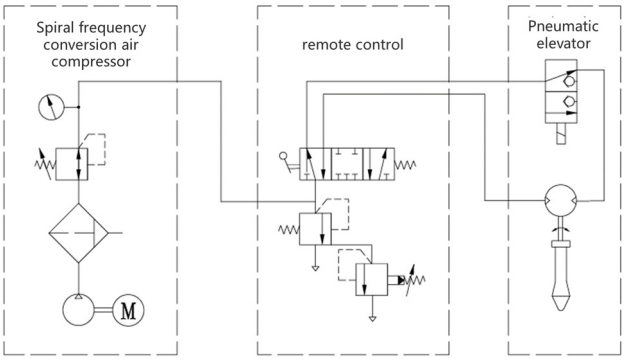

Fig 2. Pneumatic elevator pressure system schematic diagram

2.4. The Working Principle of Pneumatic Elevator

1. The work of the pneumatic elevator is mainly divided into two processes : grabbing the tubing and releasing the tubing. When the pipe is lowered, the hook hooks the lifting lug of the pneumatic elevator to lower it. Through the guiding effect of the guiding sleeve and the guiding shaft, the thread of the expansion sleeve is buckled with the tubing. When the buckle is buckled, the thread of the expansion sleeve and the tubing thread are easier to buckle and grab due to the gravity of the pneumatic elevator. At this time, the driven shaft is pushed up by the reaction force, the buffer spring is squeezed and deformed, and the impact force can be absorbed to protect the thread joint. The pneumatic motor is controlled by remote control, and the pull-in torque is output to make the thread of the expansion sleeve and the tubing thread spin together without tightening, that is, the tubing grab is completed.

2. After the completion of grasping the tubing, the power motor stops the output torque, and the control hook lifts the power elevator. After the rise, due to the gravity of the tubing, the thread of the expansion sleeve slides along the conical surface of the guide shaft, the elastic deformation of the neck of the expansion sleeve, the expansion of the external thread flap to achieve expansion, the grasping tubing is more firm, and the thread slippage is prevented.

3. Move to the top of the power tongs to prepare to release the tubing, at this time the lower end of the tubing is fixed by the power tongs, at this time the hanger does not bear the weight of the tubing, the expansion sleeve thread deformation recovery, remote control pneumatic motor reverse rotation, hook side away from the thread side rise, that is, to complete the tubing release.

4. The process of lifting the pipe is opposite to the process of lowering the pipe.

3. Finite Element Module Method

3.1. Dynamic Explicit Finite Element Analysis

In the process of buckling, the expansion sleeve faces complex loads, including tension and extrusion. Therefore, when subjected to load, the contact state between the inner wall of the expansion sleeve and the guide shaft and the thread changes alternately from separation, bonding, and sliding contact[13]. When dealing with this complex contact problem, the implicit algorithm needs to solve the global equations in each calculation step. The simulation calculation is difficult to converge, and the calculation cost is high. The explicit algorithm can simulate contact conditions and other extreme discontinuities well by solving the problem node by node without a complex iterative process. Especially in dealing with the highly nonlinear problem of three-dimensional thread contact, the explicit algorithm shows better adaptability and accuracy. Therefore, in this paper, the dynamic explicit finite element method is used to calculate the stress of the expansion sleeve when the external thread connection of the expansion sleeve is loaded.

The central difference method is used to perform explicit time integration of the motion equation, and the dynamic conditions of the next incremental step are calculated by using the dynamic conditions of one incremental step [14]. The dynamic equilibrium equation at time t is:

$$\ddot{u} = (M)^{-1}\left(P_{(t)} - I_{(t)}\right) \tag{1}$$

In the formula, u is the node displacement, M is the node mass matrix, P is the applied external force, and I is the internal stress of the element. As time goes by, it becomes explicit:

$$\dot{u}_{\left(t+\frac{\Delta t}{2}\right)} = \dot{u}_{\left(t-\frac{\Delta t}{2}\right)} + \frac{\Delta t_{(t+\Delta t)} + \Delta t_{(t)}}{2}\ddot{u}_t \tag{2}$$

$$u_{(t+\Delta t)} = u_{(t)} + \Delta t_{(t+\Delta t)}\dot{u}_{\left(t+\frac{\Delta t}{2}\right)} \tag{3}$$

According to the strain rate ε, the element strain increment dε is obtained.

According to the constitutive relationship of the material, the stress of the element is calculated as follows:

$$\sigma_{(t+\Delta t)} = f\left(\sigma_{(t)}, d\varepsilon\right) \tag{4}$$

Where σ is the element stress and ε is the element strain.

The internal force of the above element is integrated into the internal force of the node i (t + Δt), and the time t + Δt is set. Through the above process, the stress-strain law of the

model element with time can be obtained by repeated calculation.

The finite element connection control equation of thread is [15]:

$$\iiint_V \sigma_{ij}\,\delta\varepsilon_{ij}\,dV = \iint_A x_i\,\delta u_i\,dA \tag{5}$$

In the formula, σ_{ij} is the Euler stress tensor, ε_{ij} is the infinite small strain in the actual deformation, $\delta\varepsilon_{ij}$ is the virtual strain, x_i is the load vector on the surface of the unit, δu_i is the virtual displacement, V is the volume, and A is the surface area.

3.2. Dynamic Explicit Finite Element Model

The grid model of motor output shaft, connector, and driven shaft is established, as shown in Fig. 3. The upper end of the motor is completely fixed, and the rated torque of the pneumatic motor is 300N·m applied to the lower end of the driven shaft.

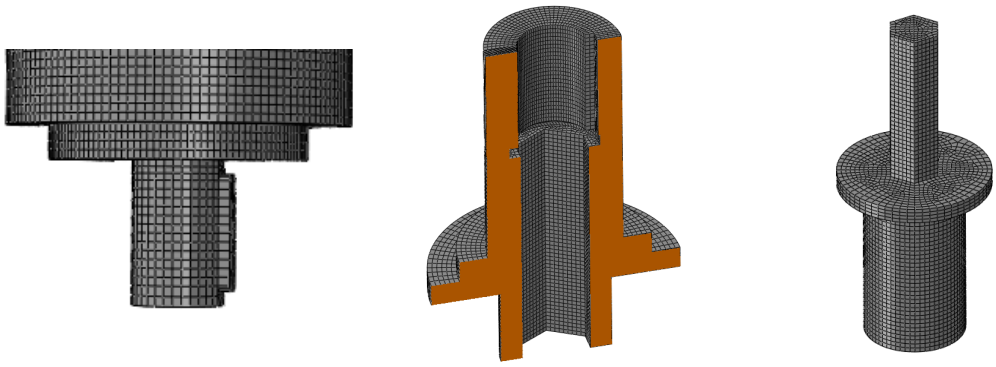

Motor output shaft connector driven shaft

Fig 3. Transmission structure grid model

The maximum lifting weight of the power elevator is 200 kg, and the maximum bearing capacity of the expansion sleeve thread is 200 kg when grabbing the tubing. The mesh model of expansion sleeves, guide shafts, and tubing is established, in which the thread connection part is locally encrypted. Set the boundary conditions, the upper end of the guide shaft is completely fixed, and the tubing gravity is applied to the lower end of the tubing. '▽' denotes completely fixed, 'G' denotes tubing gravity, and the grid model and boundary conditions are shown in Fig. 4.

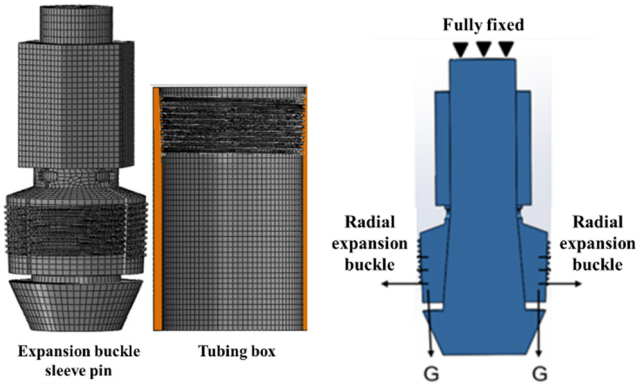

Fig 4. Mesh Model and Boundary Conditions

4. Strength Analysis of Key Structure of Pneumatic Elevator

4.1. Strength Analysis of Pneumatic Elevator Transmission Structure

The transmission torque of the elevator is transmitted, and the torsional strength of the transmission parts is tested. The output shaft of the motor and the upper end of the connector are driven by keys. The finite element calculation of the connection between the output shaft of the motor and the connector is carried out, and the rated torque of the motor is applied to 300 N · m. The calculation results are shown in Fig.5.

The material of the connector and the motor output shaft is 45 steel, the yield limit is 355 MPa, and the maximum stress value is 155 MPa, which does not reach the fatigue limit and meets the requirements of safety performance and working strength.

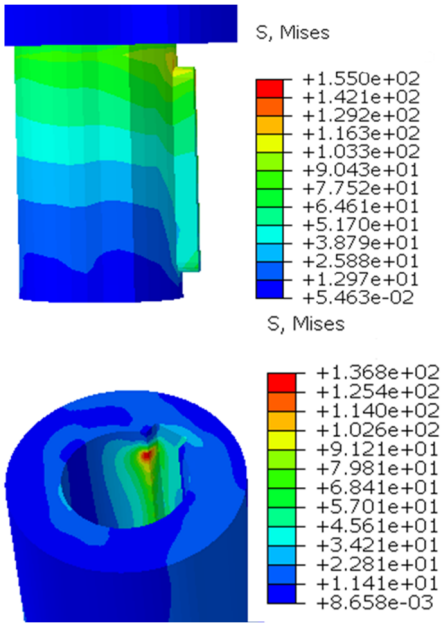

Fig 5. The stress cloud diagram of the connection between the output shaft and the upper end of the connector

The lower end of the connector and the driven shaft are transmitted through the prism, and the finite element calculation is performed on the connection between the lower end of the connector and the driven shaft. The rated torque of the motor is applied to 300N·m, and the calculation results are shown in Fig.6.

The material of the connector and the motor output shaft is 45 steel, the yield limit is 355 MPa, and the maximum stress value is 94.12 MPa, which does not reach the fatigue limit and meets the requirements of safety performance and working strength.

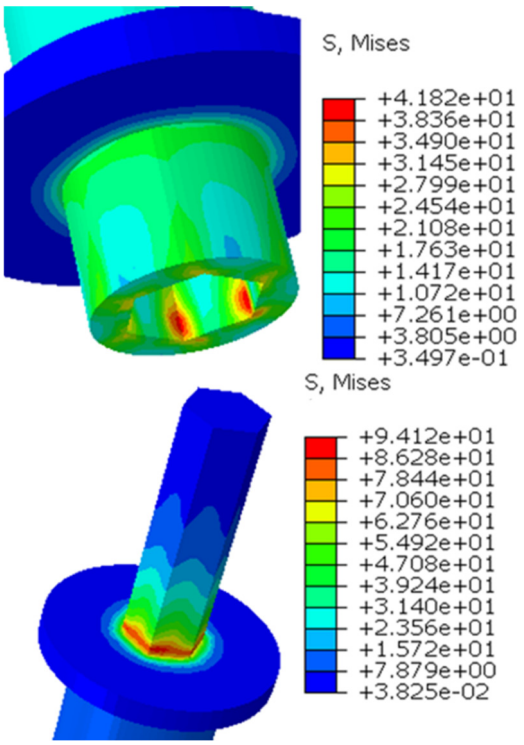

Fig 6. The stress cloud diagram of the connection between the lower end of the connector and the driven shaft

4.2. Structural Strength Analysis of Pneumatic Sling Expansion Sleeve

The structure of the expansion sleeve is composed of the expansion sleeve and the guide shaft. The force analysis of the expansion sleeve is carried out in combination with the actual working conditions, as shown in Fig.7. Under the gravity of tubing G_1, the supporting force N_1 generated by the conical surface of the guide shaft to the expansion sleeve makes the thread flap expand outward, where F_1 is the friction force.

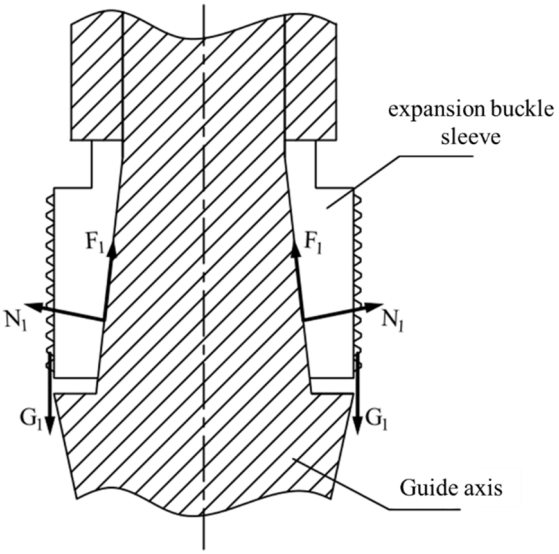

Fig 7. Expansion buckle sleeve force analysis diagram

Considering the complexity of the finished product processing and the strength of the thread, the finished product is designed as a four-thread valve expansion sleeve. The left and right sides of the neck of each thread valve are cut to shorten the arc length of the neck, so that the neck is more elastically deformed and the expansion effect is improved, as shown in Fig.8.

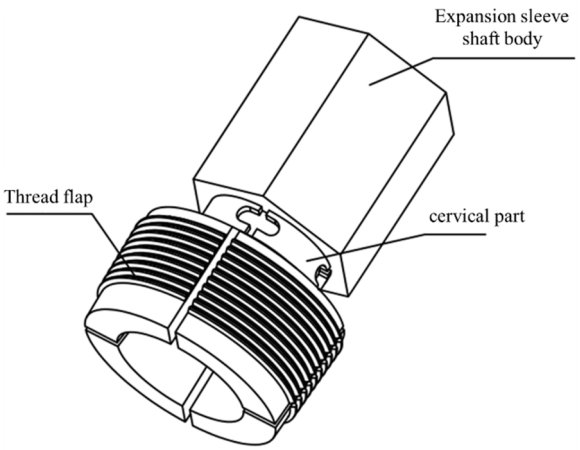

Fig 8. Structure diagram of expansion buckle sleeve

During the load-bearing process of the expansion buckle thread sleeve, the thread flap slides slightly along the conical surface of the guide shaft, and the thread flap expands slightly. At this time, the external thread of the expansion buckle sleeve and the internal thread of the tubing are squeezed to reach the limit position. The external thread of the expansion buckle sleeve, the conical surface of the guide shaft, and the neck of the expansion buckle sleeve are all subjected to load.

Fig. 9 is the finite element calculation stress cloud diagram of the expansion sleeve thread under the gravity of 200 kg of tubing. The stress is concentrated on the neck and thread of the expansion sleeve, and the maximum stress appears in the expansion sleeve thread. The material of the expansion buckle sleeve is Q345 structural steel, the yield limit is 345 MPa, and the calculated maximum stress value is 24.27 MPa, which is less than the fatigue limit of the material and meets the strength design requirements of the maximum lifting weight of 200 kg.

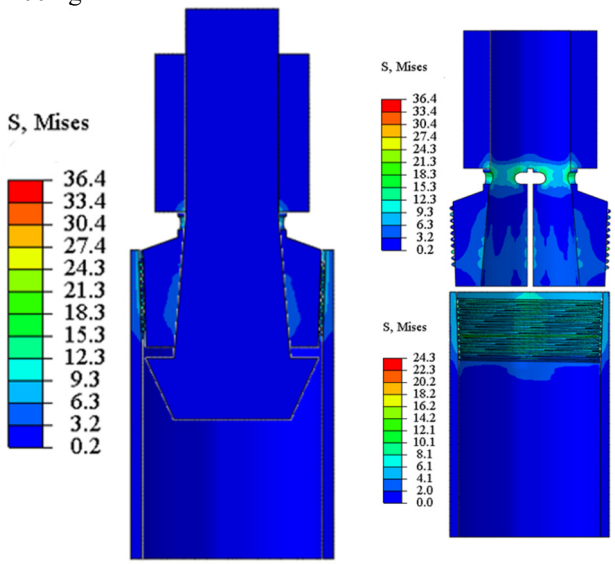

Fig 9. Expansion sleeve thread stress cloud diagram

5. Experimental Verification

In order to verify the accuracy of the finite element analysis and the reliability of the use of the pneumatic elevator, the functional test and load test of the pneumatic elevator were carried out in the test field of Sichuan Shengnuo Oil and Gas Engineering Technology Service Co., Ltd.

The pneumatic elevator obtained by structural design and strength check can output a rated torque of 300 N·m under the action of a spiral variable frequency air compressor, which

meets the maximum rated torque requirement of 300 N·m and meets the power demand. The pneumatic elevator meets the requirements of less than 200 kg in weight and realizes ground operation control. It can control the lifting motion of the automatic buckle power system with a hand-held remote controller and control the motor to drive the buckle unloading operation.

Experiments were carried out in the field environment: under the remote control of workers, the grabbing, fastening, and unloading of 73 mm gas-sealed tubing were successfully completed, as shown in Fig.10. The whole operation process is completed stably, which meets the requirements of the buckle operation of the 73 mm gas seal buckle tubing. The operator is away from the remote control operation of the elevator, which ensures the safety of the operator. The follow-up experiment lasted for several months, and the buckle operation was still completed successfully.

Fig 10. Field test diagram

6. Conclusion

(1) According to the design parameters, the maximum lifting weight is 200 kg, and the design and strength check of a new type of pneumatic lifting card are completed. The lifting card replaces the manual operation of the tubing with a pneumatic motor to realize the grabbing and spin-off release of the tubing, which solves the problems of complicated, easy leakage and the high environmental requirements of the traditional hydraulic lifting card. It has the advantages of a simple structure, low cost, and stable operation in harsh environments.

(2) Through the strength analysis of the finite element software, the technical scheme of the hanging card is feasible, the design structure is simple, and it can be applied to a wide range of pipe diameters. Workers can operate remotely, replacing manual buckles and improving safety.

(3) The functional test and load test were carried out to verify the correctness of the finite element analysis and calculation, and the normal operation of the functions of the pneumatic elevator was verified. The data show that the pneumatic elevator meets the requirements of field use.

References

[1] Zhang, Q. J., Cheng, L., Yang, X., Shan, B., & Zhang, T. (2023). Development of a Fully Automatic Hydraulic Elevator. Mechanical Engineer, (12), 113-115, 119.

[2] Wang, R. Z., Wang, S. G., Yan, J. Z., Liu, F. G., Liu, C. J., & Song, C. (2021). Development and Structural Strength Analysis of Hydraulic Elevator. Oil Field Equipment, 50(6), 38-44.

[3] Kang, X. D., Yu, B., Yin, H., Wang, T., & Shi, M. J. (2022). Development of a New Type of Automatic Rotating Electric Elevator Device. Modern Manufacturing Technology & Equipment, 58(10), 161-164.

[4] Geng, Y. G., Pei, Y. S., Gu, Q. F., Huang, S., Sun, L. H., & Wang, J. W. (2016). Remote Control Technology for Single-Elevator Tripping Operations. Oil Drilling & Production Technology, 38(5), 709-712.

[5] Wang, Q., & Gao, G. Q. (2018). Design and Analysis of a Mechanized Elevator Transfer Device. Machine Design and Manufacturing Engineering, 47(6), 53-55.

[6] Chen, K. Y. (2018). Finite Element Analysis of an Ultra-Deep Well Elevator. Horizon of Science and Technology, (29), 235-236.

[7] Han, F., Li, X. M., Ji, Y. Z., Xu, Y. T., & Yang, Z. X. (2012). Design and Finite Element Analysis of a Rotary Casing Elevator. China Petroleum Machinery, (9), 9-11.

[8] Jiang, L. H., Zhou, B., Tan, Y. G., Huang, A. Y., Wang, X., & Wang, L. B. (2017). Development of an Automatic Rotating Elevator. Oil Drilling & Production Technology, 39(6), 791-794.

[9] Cui, H. P. (2019). Mechanical Analysis and Calculation of Hydraulic Elevator. Mechanical & Electrical Engineering Technology, 48(7), 44-46, 276.

[10] Wang, J. B., Zhang, X. Y., & Li, J. (2019). Safety Performance Analysis and Improvement Measures for Locking Ring Type Elevator. Chemical Enterprise Management, (19), 131-132.

[11] Niu, W. J., Bai, Y. T., Yu, Y. Q., Wang, Y. A., & Xu, G. H. (2016). Development of a New Split-Type Powered Elevator. Journal of Donghua University (Natural Science Edition), 42(4), 512-517.

[12] Chen, D., Zhou, J. L., Xu, B. B., & Zhang, K. (2022). Structural Optimization Design of CDZ500 Drill Pipe Elevator. Machine Design and Manufacturing, 374(4), 30-32, 36.

[13] Zhu, X., Lin, D., & Li, J. (2016). Failure analysis and structure optimization of the connecting thread of driving shaft in positive displacement motor. Advances in Mechanical Engineering, 8(6), 1687814016652313.

[14] Z. Zhuang, X.-C. You, J.-H. Liao, Finite element analysis and application of ABAQUS, Tsinghua University Press, Beijing, China, 2009.

[15] Yang, Y., Ke, Y. L., & Dong, H. Y. (2006). Finite element simulation of high-speed cutting. ACTA AERONAUTICA ET ASTRONAUTICA SINICA-SERIES A AND B-, 27(3), 531.